New Materials & Devices
Building Blocks for Future

Stabilization of the ANATASE *phase* and *Structural modification* of nanostructured TiO_2 *via* DEFECT ENGINEERING and DOPING: synthesis, characterization and photocatalytic properties

Abstract

Nanostructured TiO_2 is the most studied photocatalytic semiconductor oxide, but it has two main limitations. It absorbs light only in the UV region, and its photogenerated electron-hole pairs recombine quickly. The anatase phase is more efficient than rutile because its charge carriers are more mobile. This study tested ways to stabilize anatase and modify the optical and structural properties of TiO_2 doping with Al^{3+} and In^{3+}, synthesis under an O_2 atmosphere, and adjusting the pH and the citric acid:cation ratio. The powders were prepared by the modified polymeric precursor method. They were characterized by thermal analysis, XRD with Rietveld refinement, Raman spectroscopy and SEM.

Sample — Polymeric Precursor Method (PPM)

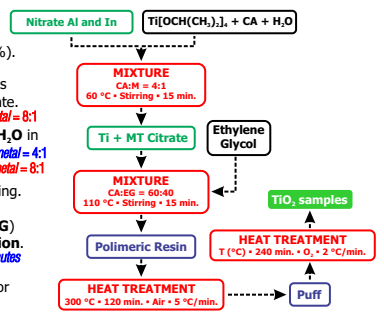
❶ The metal sources in the synthesis were Titanium tetraisopropoxide, **Ti[OCH(CH$_3$)$_2$]$_4$** (Sigma-Aldrich, 97%), and Aluminum nitrate and Indium nitrate (Sigma-Aldrich, >98%).

❷ **Ti[OCH(CH$_3$)$_2$]$_4$** was dissolved in an citric acid (**CA**) aqueous solution at **100º C** under constant stirring to obtain the Ti citrate. *CA:metal = 4:1 CA:metal = 8:1*

❸ Al citrate was obtained by the dissolution of the **Al(NO$_3$)$_3$·9H$_2$O** in distiled water. After a complete dissolution, **CA** was added. *CA:metal = 4:1 CA:metal = 8:1*

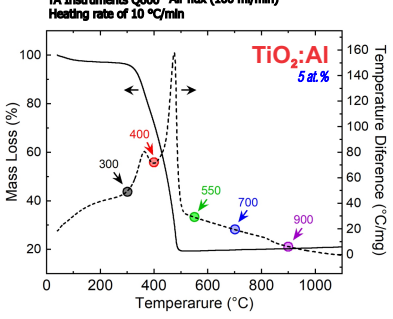
❹ Both citrates were than mixed at **60 °C** under constant stirring. After the formation of a completely homogenous solution the temperature was raised up to **~110 °C** and ethylene glycol (**EG**) was added to promote a **polymerization by polyesterification**. *CA:EG = 60:40 ~ 15 minutes*

❺ The polymeric precursor resin was heat treated at **300° C** for **2 h in Air** at heating rate of **5° C/min**.

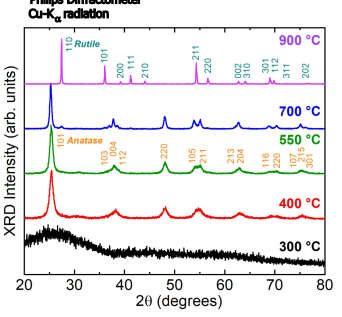


Results ❶ *Thermal* Analysis

TG+DTA
TA Instruments Q600 Air flux (100 ml/min)
Heating rate of 10 °C/min



XRD
Philips Diffractometer
Cu-K$_\alpha$ radiation



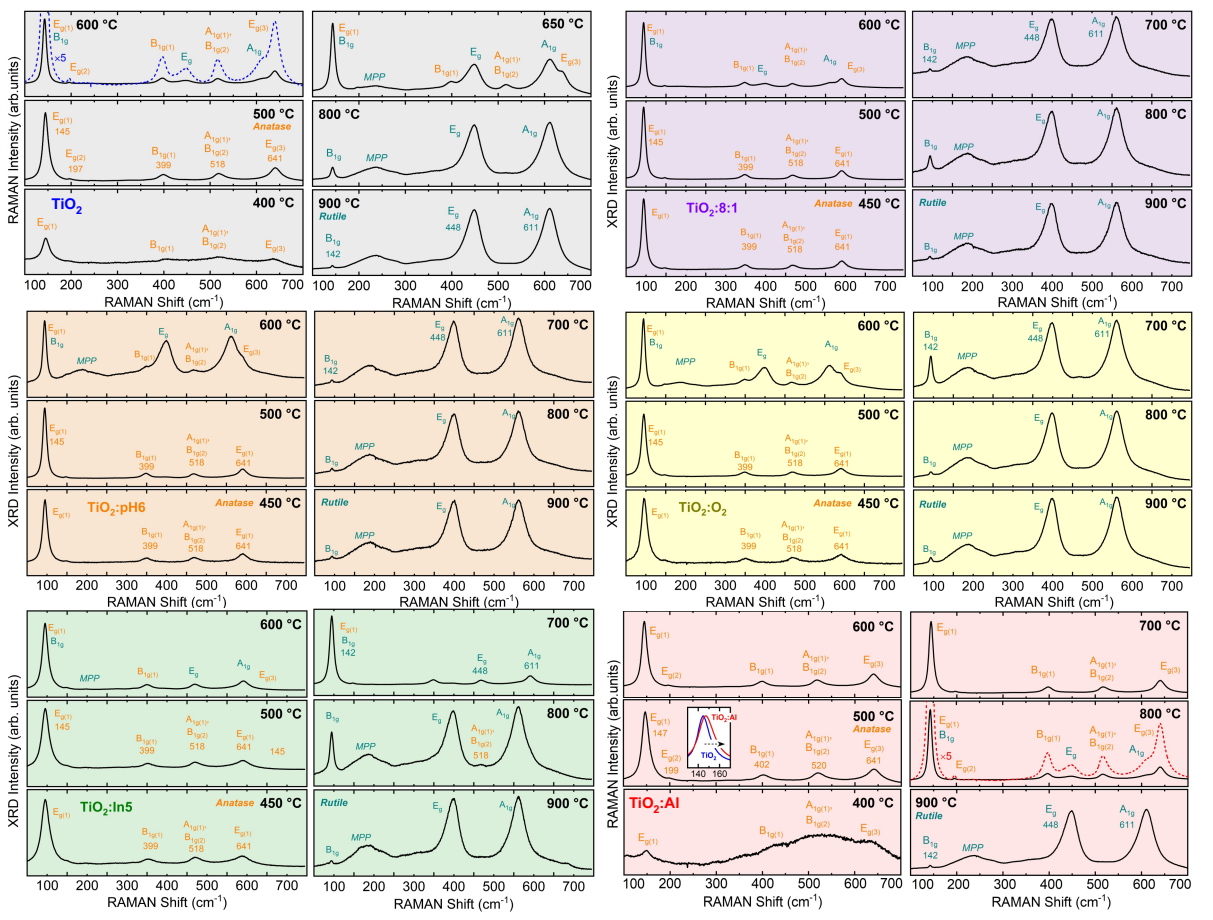
❶ Evaporation of residual water. **5%**
❷ Burning of organic material and crystallization in the anatase phase. **87%**

✔ **Al** does not substantially **changes the thermal and chemical kinetics** as compared to the obtained, and previous discussed, for the TiO_2 sample.

✔ The observation of a small amount of rutile phase at low temperatures and the broad range in temperature for the conversion of the anatase to the rutile structure reveals the **metastable** character of the **anatase TiO_2 structure**.

✖ **Particle size dependence**
Nanoscale → Anatase
Micrometric → Rutile
Surface free energy related

Results ❷ RAMAN



Horiba IHR-550 micro-Raman backscattering geometry / 532 nm
Spot size: 2 mm
Power: 1 mW

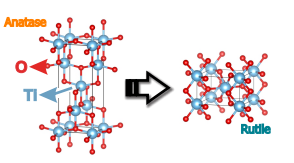
RAMAN
Vibrational Modes
Anatase:
$E_{g(1)}$, $E_{g(2)}$, $B_{1g(1)}$, $A_{1g(1)}$, $B_{1g(2)}$ and $E_{g(3)}$.
Rutile:
B_{1g}, E_g and A_{1g}.

✔ **No presence of any secondary phase.**

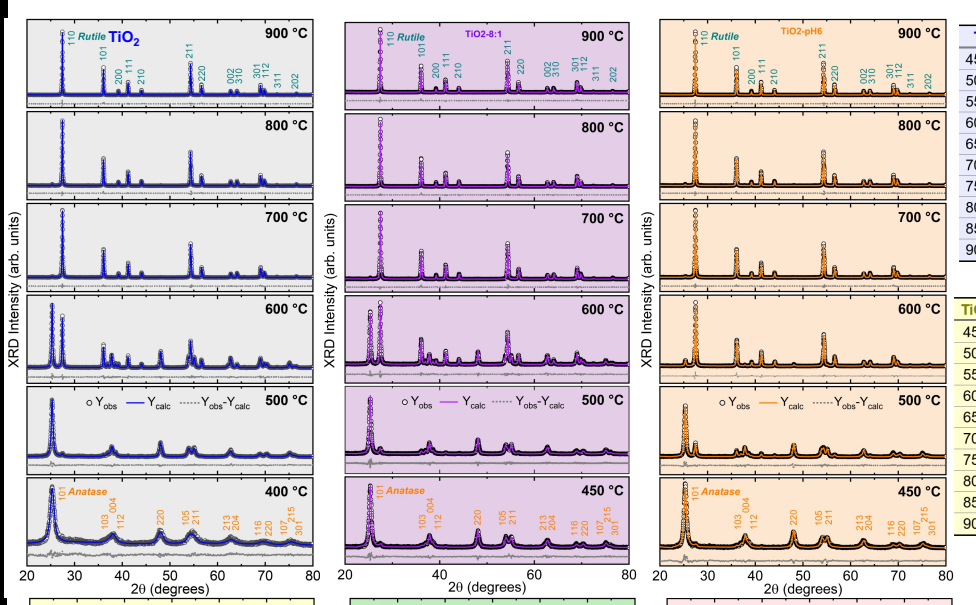
✖ Al^{3+}-doping of the TiO_2 lattice at Ti^{4+} sites
Substitutional doping

✔ Significant **decrease in the crystallinity** for these **Al-doped samples**.

✔ **Small dopant ionic radius** produces large crystal lattice deformations (lattice contraction) **inhibiting the anatase-rutile transition**.
$r_{Al} = 0.535$ Å $< r_{Ti} = 0.605$ Å



Results ❸ XRD + RIETVELD GSAS II / EXPGUI



TiO_2	Anatase	Rutilo	χ^2	R_{wp} (%)	R_p (%)
450 °C	100(1)	-	1.41	15.68	11.89
500 °C	95.3(2)	4.7(1)	1.25	14.71	10.17
550 °C	83.2(5)	16.8(1)	1.25	15.02	10.41
600 °C	52.5(1)	47.5(1)	1.21	14.61	09.78
650 °C	10.8(1)	89.2(3)	1.29	15.63	10.03
700 °C	1.2(5)	98.8(4)	1.34	15.59	09.85
750 °C	2.38(7)	97.62(8)	1.27	15,62	10.03
800 °C	1.43(5)	98.57(5)	1.28	15.90	09.90
850 °C	-	100	1.33	15.91	09.82
900 °C	-	100	1.40	16.26	10.28

TiO_2:8:1	Anatase	Rutilo	χ^2	R_{wp} (%)	R_p (%)
450 °C	92.81(6)	7.18(2)	1.39	17.26	12.12
500 °C	88.4(1)	11.5(2)	1.35	16.80	11.70
550 °C	73.8(1)	26.1(2)	1.39	17.65	12.61
600 °C	41.6(1)	58.3(1)	1.28	16.51	11.16
650 °C	15.7(1)	84.28(7)	1.31	17.02	10.89
700 °C	0.94(6)	99.05(4)	1.26	16.49	10.34
750 °C	0.10(2)	99.89(3)	1.38	17.01	10.91
800 °C	-	100	1.21	16.24	09.76
850 °C	-	100	1.35	17.23	10.57
900 °C	-	100	4.05	29.99	22.90

TiO_2:pH6	Anatase	Rutilo	χ^2	R_{wp} (%)	R_p (%)
450 °C	94.6(1)	5.3(3)	1.51	16.77	12.46
500 °C	76.4(2)	23.5(2)	1.43	16.46	11.63
550 °C	43.0(1)	56.9(1)	1.34	16.54	11.39
600 °C	7.5(1)	92.47(4)	1.32	16.52	10.85
650 °C	0.27(4)	99.72(1)	1.36	16.90	10.54
700 °C	0.09(2)	99.91(2)	1.25	16.18	10.24
750 °C	-	100	1.36	16.88	10.93
800 °C	-	100	1.32	16.71	10.29
850 °C	-	100	1.34	17.18	10.47
900 °C	-	100	1.49	17.75	11.25

TiO_2:O_2	Anatase	Rutilo	χ^2	R_{wp} (%)	R_p (%)
450 °C	100	-	1.25	15.81	12.00
500 °C	99.91(4)	0.08(1)	1.30	15.91	12.12
550 °C	93.87(5)	6.1(2)	1.39	16.74	12.00
600 °C	76.6(1)	23.3(3)	1.83	22.07	17.41
650 °C	14.4(2)	85.6(1)	1.32	17.05	11.60
700 °C	4.17(1)	95.8(1)	1.37	18.35	12.12
750 °C	0.22(4)	99.77(5)	1.36	18.51	11.92
800 °C	0.02(3)	99.97(1)	2.77	24.18	17.55
850 °C	-	100	1.35	17.11	11.49
900 °C	-	100	1.47	17.60	11.62

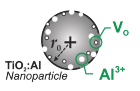
TiO_2:In	Anatase	Rutilo	χ^2	R_{wp} (%)	R_p (%)
450 °C	100	-	3.11	16.35	12.78
500 °C	100	-	2.96	15.45	12.22
550 °C	98.02	1.97	3.15	16.06	12.67
600 °C	96.51	3.49	3.59	16.79	13.03
650 °C	94.89	5.10	3.42	17.80	13.30
700 °C	87.38	12.61	4.94	20.60	15,19
750 °C	60.77	39.22	8.95	27.71	21.47
800 °C	1.52	98.47	14.85	35.49	29.08
850 °C	-	100	15.59	36.67	27.97
900 °C	-	100	14.04	34.96	24.63

TiO_2:Al	Anatase	Rutilo	χ^2	R_{wp} (%)	R_p (%)
450 °C	100	-	1.43	16.08	11.85
500 °C	100	-	1.46	15.81	11.46
550 °C	100	-	1.50	16.13	11.68
600 °C	97.39	2.61	1.40	15.55	11.20
650 °C	96.8	3.2	1.39	15.08	11.89
700 °C	95.1	4.9	1.25	14.78	11.79
750 °C	92.4	7.6	1.18	14.33	09.70
800 °C	56.1	4.4	1.31	15.40	10.08
850 °C	100	-	1.28	15.49	09.72
900 °C	100	-	1.35	15.82	10.04

✔ **No presence of any secondary phase.**

✔ Significant **decrease in the crystallinity** for these Al-doped samples and a **decreasing of the size of the nanoparticles**.

✖ **Al^{3+} and In^{3+} substitutional doping of the Ti^{4+} sites, mainly at the surface of the nanoparticles.**

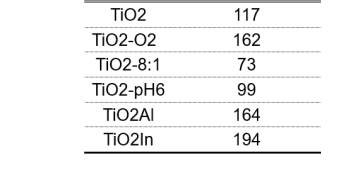


✔ With the addition of the **Al** and **In**, the diffraction peak associated with **the rutile phase disappears** at low temperatures.
Al^{3+}-doping of the anatase TiO_2 structure

✔ **Al^{3+} and In^{3+} substitutional doping** disfavor the anatase-rutile transition.
Favoring the V_o via charge compensation process

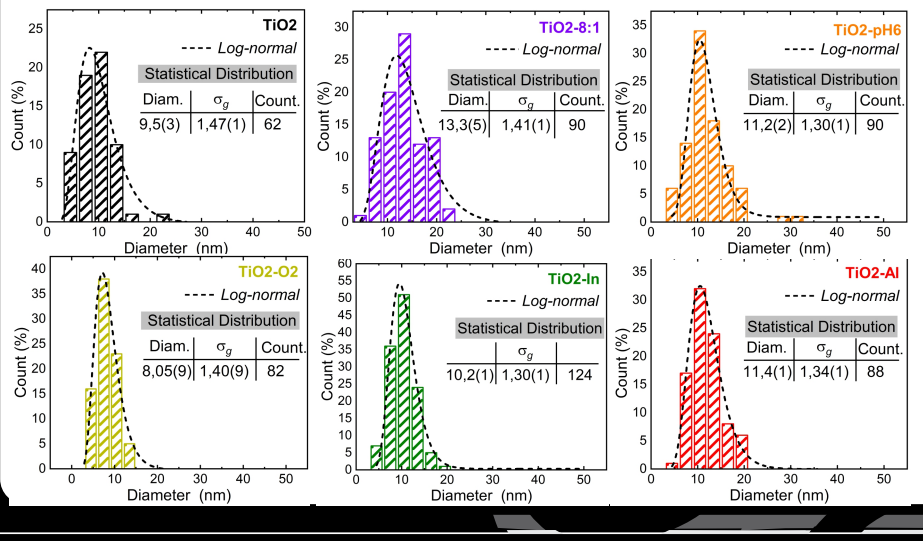
✖ **Al^{3+} substitutional doping** imposes mechanical restrictions **inhibiting the structural conformations** necessary for the phase transition, thus leading to its inhibition.

✖ **In^{3+} substitutional doping** imposes mechanical restrictions but we have **two secondary phases at high temperatures**



Samples	Activation Energy
TiO2	117
TiO2-O2	162
TiO2-8:1	73
TiO2-pH6	99
TiO2Al	164
TiO2In	194

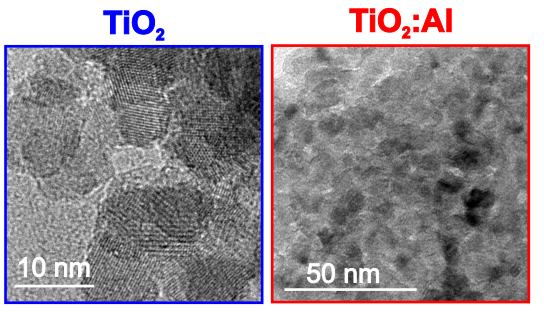
Results ❹ Morphology and Elemental Characterization TEM



Quanta FEG 3D FEI / EDS

- All samples follow a log-normal distribution, with mean diameters of 8–13 nm.
- **Synthesis**: O_2 gave the smallest particles (8.05 nm) and 8:1 the largest (13.3 nm). pH 6 gave the narrowest distribution (σ_g = 1.30).
- **Doping**: In and Al slightly increased the mean size (10.2 and 11.4 nm vs. 9.5 nm for pure TiO_2) and narrowed the distribution (σ_g 1.30 – 1.34 vs. 1.47).
- **HRTEM**: pure TiO_2 shows clear lattice fringes, so the particles are

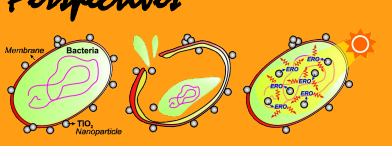
TiO_2 | TiO_2:Al



Conclusions

In this work, we present the study on the preparation and structural characterization of nanostructured samples of TiO_2 doped with Al^{3+} and In^{3+}. The polymeric precursor method was used for preparation. The reaction kinetics of the precursor material were determined by thermal analysis, thermogravimetry (TG), differential thermal analysis (DT), and X-ray diffraction (XRD). From the results obtained, we determined the preparation parameters of TiO_2. In the structural characterization of the prepared powders, we also used the XRD technique, now associated with the Rietveld structural refinement technique, including Raman scattering spectroscopy. The experimental results for both sets of samples indicate the incorporation of the dopant, Al^{3+} and In^{3+}, into the TiO_2 matrix without the formation of undesirable secondary phases, such as dopant oxides or ternary phases between Ti, Al, and O. Here, we have evidence that the dopants are mostly located on the surface of the TiO_2 nanoparticle. The addition of Al^{3+} to the TiO_2 structure introduces lattice deformations (contraction of lattice parameters) and potentially point defects (oxygen vacancies) that inhibit the anatase-to-rutile phase transition. The phase transition energy increases.

Perspectives



Vinicius Justino Pimenta[1], Thainá de Paula Teixeira[2], Hugo B. de Carvalho[2]
[1]Federal University of Ouro Preto, Ouro Preto, MG, Brazil, [2]Federal University of Alfenas, Alfenas, MG, Brazil
vinicius.pimenta@aluno.ufop.edu.br

Acknowledgements:
This study was financed in part by the Coordenação de Aperfeiçoamento de Pessoal de Nível Superior - Brasil (CAPES), Universidade Federal de Ouro Preto (UFOP), and Rede Temática em Engenharia de Materiais (REDEMAT).